

Short-range Visible Light Positioning Based on Angle of Arrival for Smart Indoor Service

Yong Up Lee* and Seop Hyeong Park†

Abstract – In visible light (VL) positioning based on angle of arrival (AOA) estimation for smart indoor service, the AOA parameters obtained at the receiver has sometimes a random and distributed angle form instead of a point angle form due to the multipath transfer of the actual visible light and short positioning distance. The AOA estimation of a VL signal with a random and parametric distributed angle form may give incorrect AOA parameter estimates, which may result in poor VL positioning performance. In this paper, we classify the AOA parameters of the received VL signal into three forms according to the actual positioning channel environment and consider the short-range VL positioning method. We propose a subspace-based AOA parameter estimation technique and a data fusion method, and analyzed the proposed method by simulation and the measurement of the real VL channel characteristics.

Keywords: Visible light communication, Indoor positioning, Angle of arrival, Visible light channel, Data fusion

1. Introduction

In the era of the Fourth Industry Revolution, various smart indoor (e.g., home, building, factory, or farm) services are expected to be provided by VL positioning technique instead of conventional wireless ones because of high safety and security characteristics owing to visible feature. Researches on VL positioning have been actively carried out for better smart indoor services [1-3].

In conventional VL positioning, the position of the receiver or target is simply determined by fusing the parameter estimates, which are obtained by estimating the unknown parameters (e.g. received signal strength, time-of-arrival, or AOA) at the receiver. The estimation of the received signal strength parameter is severely affected by the amplitude distortion due to fading in the VL channels, and the time-of-arrival parameter estimation requires time synchronization of the receivers [4-5]. VL positioning based on the AOA parameters as shown in Fig. 1 is preferred to that based on the received signal strength or time-of-arrival parameter because AOA parameters have no relevance to amplitude distortion or time synchronization.

Conventional VL positioning based on AOA parameters [6] has the following procedure: the AOA parameters are obtained by the reception of the VL signals and the array signal processing [7] at the receiver with photodiode array, and the position of the receiver is determined from fusing the AOA estimates and the known positions of the transmitters.

However, the AOA parameters estimated at the receiver may be a random and distributed angle form under the real channel environment [8] of the VL positioning for smart indoor service rather than a deterministic and point angle form. In the short-distance or micro-scale VL positioning for smart indoor services where the positioning distance is several to several ten times the photodiode array size of the receiver, the VL positioning based on AOA parameters of a random and distributed angle form stare us in the face because of the multipath transfer and the short positioning distance of the VL positioning. Then, the conventional parameter estimation techniques may give us a poor performance under the positioning environment with the AOA of the random and distributed angle form. On the other hand, the AOA parameters in long-range VL positioning are expected to be a point angle form.

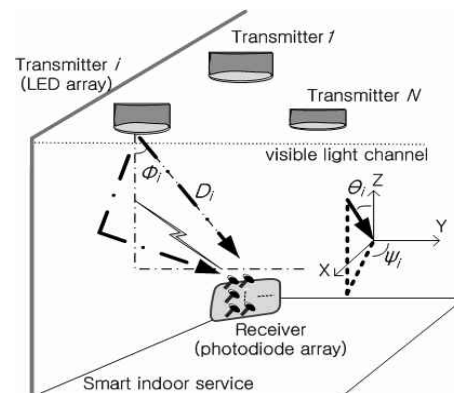


Fig. 1. The channel environment of the VL positioning methodology based on the AOA parameter estimation for the smart indoor service

† Corresponding Author: Dept. of Electronic Engineering, Hallym University, Korea. (spark@hallym.ac.kr)

* Dept. of Electronic Engineering, Hallym University, Korea. (yulee@hallym.ac.kr)

Received: June 7, 2017; Accepted: December 18, 2017

2. VL Positioning Method for Smart Indoor Service

2.1 AOA under Real VL positioning channel

Fig. 2 shows three forms of the AOA parameters of the VL signals acquired at the receiver when the VL signal is generated by the VL transmitters. According to previous VL channel studies [9-11], the VL channel between transmitter and the receiver has not only a direct line of sight (LOS) path but also multiple reflected paths similar to wireless channel.

Fig. 2(a) shows a deterministic point angle form where each AOA has a single point value and both the direct LOS path and the multiple reflected path signals have the same point angle values, i.e., $\theta_i(t) = \theta_i(s) = \theta_i, t \neq s$. It is expected that the long-range VL positioning, where the positioning distance is compared with the hundreds or thousands of times the photodiode array size of the receiver, could give us the point angle form of Fig. 2(a). In this case, the impulse response is written as follows: $h(\theta) =$

$\sum_{i=1}^N h_i \delta(\theta - \theta_i)$, where h_i and θ_i are the path amplitude and the AOA from the i -th transmitter, respectively, N is the number of transmitters and $\delta(\cdot)$ is a delta function. In conventional VL positioning based on the AOA parameters, the AOA parameters have been assumed to be a point and deterministic angle form up to now.

As an extension of a previous study [12], we consider the real VL channel characteristics to improve VL positioning accuracy. However, the real VL channel under micro-scale or short-distance VL positioning has such channel characteristics that the AOA of the direct LOS path signal is quite *different* from that of the multiple reflected

path signals. In that case, it is *natural* that the AOA is assumed to be a random and distributed angle form, i.e., a random distribution of the point angle form with the specific probability density function (PDF) instead of point and deterministic angle values. The AOA acquired at the receiver can also be diverse distributed forms (e.g., the nonparametric function of Fig. 2(b) or the parametric function of Fig. 2(c)). The angular impulse response by the VL signal of the random and distributed angle form is written as follows:

$$h(\theta) = \sum_{i=1}^N \sum_{k=1}^Q h_{ik} \delta(\theta - \theta_i - \omega_{ik}), \quad (1)$$

where h_{ik} and ω_{ik} are the k -th path amplitude and the AOA generated from the i -th transmitter, respectively, θ_i is the center AOA parameter with a random and distributed form, θ is the AOA with a random process with a specific PDF, and Q is the number of multipath signals within one cluster.

If a uniform linear photodiode array is used at the receiver as shown in Fig. 3, then the arrival time difference of the i -th source at two different sensors, the first and the l -th sensor, is given as $T_{li} = d(l-1)\sin\theta_i / c$, where d is the distance between two adjacent sensors and c is the speed of light.

After some calculation [7], the channel impulse response at the l -th sensor is given as

$$h_l(t) = \sum_{i=1}^N \sum_{k=1}^Q h_{ik}(t) e^{-j\pi d(l-1)\sin(\theta_i + \omega_{ik})}. \quad (2)$$

2.2 Signal model

In VL positioning based on AOA parameter estimation, the D -bit signal generated from the transmitter is given

$$x(t) = \sum_{k=0}^{D-1} A_k p(t - kT_b), \quad (3)$$

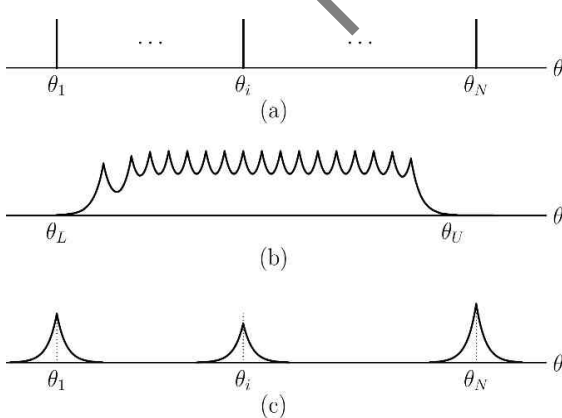


Fig. 2. Three forms of the AOA parameter observed at the receiver under the real VL positioning channel (a) a point angle form (b) a random and nonparametric distributed angle form (c) a random and parametric distributed angle form

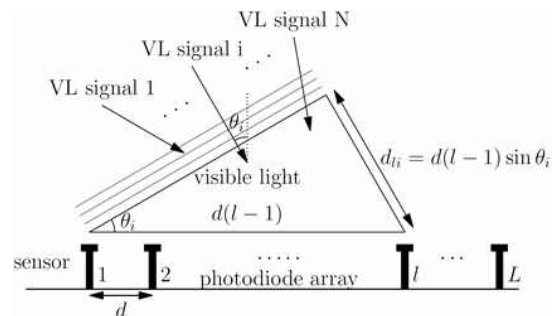


Fig. 3. The reception process of the VL signals acquired at the receiver of the photodiode array of uniform linear array sensor

where A_k is the signal intensity with ± 1 , $p(\cdot)$ is a digital pulse shape, and T_b is a bit duration. The transmitted power of an LED array is $p_{\text{LED}} = x^2(t)$, and the transferred power through VL channel is $p_T = I(\phi) p_{\text{LED}}$, where $I(\phi)$ is the light intensity of an LED array at an irradiance angle ϕ . Since the visible light signal of an LED array is usually assumed to be of diffuse nature with Lambertian emission, the light intensity is given as $I(\phi) = [(1+m)/2\pi] \cos^m \phi$, where m is an emission order [9].

If the VL signals generated from N transmitters are transferred to the positioning channel and N VL signals of the random and parametric distributed angle forms are observed at the receivers, the l -th received signal at the photodiode array of the receiver is obtained as follows,

$$y_l(t) = \sum_{i=1}^N \sum_{k=1}^Q h_{ik}(t) e^{-j\pi d(l-1)\sin(\theta_i + \omega_{ik})} x(t - \tau_{ik}) + \eta_l(t), \quad (4)$$

$$1 \leq l \leq L,$$

where $\eta_l(t)$ is the noise at the l -th sensor of the photodiode array. To represent Eq. (4) in a form of vector equation, let us define $\mathbf{y}(t) = [y_1(t) \cdots y_L(t)]^T$ and $\boldsymbol{\eta}(t) = [\eta_1(t) \cdots \eta_L(t)]^T$, where T is the vector transpose operator. It is natural that the VL positioning channel in Eq. (4) has flat fading characteristic (i.e., approximately zero path time difference) like indoor wireless channel. Then, Eq. (4) can be rewritten as

$$\mathbf{y}(t) = \sum_{i=1}^N x(t - \tau_i) \sum_{k=1}^Q h_{ik}(t) \mathbf{a}(\theta_i + \omega_{ik}) + \boldsymbol{\eta}(t), \quad (5)$$

where $\mathbf{a}(\theta) = [1 \cdots e^{-j\pi d(l-1)\sin\theta} \cdots e^{-j\pi d(L-1)\sin\theta}]^T$ is the steering vector. For investigation of the AOA of the received VL signal, we here assume the mean received signal amplitude to be $\tilde{x}(t - \tau_i) = \bar{h}_i x(t - \tau_i)$, where $\bar{h}_i = \sum_{k=1}^Q h_{ik}(t)$. Then, Eq. (5) is given as

$$\mathbf{y}(t) = \sum_{i=1}^N \tilde{x}(t - \tau_i) \sum_{k=1}^Q \mathbf{a}(\theta_i + \omega_{ik}) + \boldsymbol{\eta}(t). \quad (6)$$

2.3 Subspace-based AOA parameter estimation

To estimate the AOA parameters of the random and parametric distributed angle form in short-range VL positioning, it is natural that the reception process of the VL signal at the photodiode array receiver is described by a new steering vector operation connoted the random and distributed characteristic of the directional arrival. Then we consider the mean operation of the steering vector as follows

$$\mathbf{b}(\theta, \rho_\theta) \equiv E\{\mathbf{a}(\theta)\} = \frac{1}{2\pi} \int_0^{2\pi} \mathbf{a}(\theta) p(\theta) d\theta \quad (7)$$

where $E\{\cdot\}$ is an expectation operator, $\mathbf{a}(\theta)$ is the conventional steering vector, $p(\theta)$ is the PDF of the centre AOA parameter θ , and ρ_θ is the spread AOA parameter of the received VL signal of the random distributed angle form.

We can think of various probability distribution functions for $p(\theta)$, but we here consider the Laplace probability distribution, $p(\theta) = \frac{1}{\sqrt{2\rho}} e^{-|\sqrt{2}/\rho|}$, for random and parametric distributed AOA in short-range VL positioning. Then the mean steering vector is obtained as follows:

$$\mathbf{b}(\theta_i, \rho_{\theta_i}) = b_1(\theta_i, \rho_{\theta_i}) \cdots b_L(\theta_i, \rho_{\theta_i}) \cdots b_L(\theta_i, \rho_{\theta_i})^T, \quad (8)$$

where $b_l(\theta_i, \rho_{\theta_i}) = \frac{1}{1 - j l \rho_{\theta_i} / \sqrt{2}} a_l(\theta_i)$ and

$$a_l(\theta_i) = e^{-j\pi d(l-1)\sin\theta_i}.$$

In a short-range VL positioning environment for smart indoor service as in Fig. 1, the signal processing at the receiver by the mean steering vector in Eq. (8) is represented as follows:

$$\mathbf{y}(t) = \sum_{i=1}^N \mathbf{b}(\theta_i, \rho_{\theta_i}) \tilde{x}(t - \tau_i) + \boldsymbol{\eta}(t). \quad (9)$$

In order to apply the subspace-based AOA parameter estimation technique to the signal acquisition process of Eq. (9), the covariance matrix of the received VL signal is introduced as

$$\begin{aligned} \mathbf{R}_{yy} &= E\{\mathbf{y}(t)\mathbf{y}^H(t)\} \\ &= \sum_{i=1}^N \sum_{k=1}^N r_x(\tau_i - \tau_k) \mathbf{b}(\theta_i, \rho_{\theta_i}) \mathbf{b}^H(\theta_k, \rho_{\theta_k}) + \sigma_\eta^2 \mathbf{I} \end{aligned} \quad (10)$$

where $r_x(\tau_i - \tau_k) = E\{x_i(t - \tau_i)x_k(t - \tau_k)\}$, $\sigma_\eta^2 \mathbf{I} = E\{\boldsymbol{\eta}(t)\boldsymbol{\eta}^H(t)\}$ and H is a complex conjugate transpose operator. Let $\lambda_1 \geq \lambda_2 \geq \cdots \geq \lambda_L$ be the eigenvalues and $\mathbf{e}_1, \mathbf{e}_2, \cdots, \mathbf{e}_L$ be the corresponding eigenvectors of \mathbf{R}_{yy} . Define $\mathbf{G} = [\mathbf{e}_{N+1} \cdots \mathbf{e}_L]$. Then, $\text{Span}\{\mathbf{G}\}$ is the noise subspace. We obtain the following relationship:

$$\mathbf{R}_{yy} \mathbf{G} = \sum_{i=1}^N \sum_{k=1}^N r_x(\tau_i - \tau_k) \mathbf{b}(\theta_i, \rho_{\theta_i}) \mathbf{b}^H(\theta_k, \rho_{\theta_k}) \mathbf{G} + \sigma_\eta^2 \mathbf{I} \mathbf{G}$$

$$= \sigma_\eta^2 \mathbf{G}. \tag{11}$$

Then the null spectrum of the AOA parameter estimation in a short-range VL positioning environment by the subspace-based estimation technique is given as

$$\mathbf{b}(\theta, \rho_\theta) \mathbf{G} \mathbf{G}^H \mathbf{b}^H(\theta, \rho_\theta) = 0, \tag{12}$$

where $(\theta, \rho_\theta) \in \{(\theta_1, \rho_{\theta_1}), \dots, (\theta_N, \rho_{\theta_N})\}$.

In real positioning environments, the sample null spectrum is obtained as $p(\theta, \rho_\theta) = \mathbf{b}(\theta, \rho_\theta) \hat{\mathbf{G}} \hat{\mathbf{G}}^H \mathbf{b}^H(\theta, \rho_\theta)$ instead of the null spectrum in Eq. (12), where $\hat{\mathbf{G}} = [\hat{e}_{N+1} \dots \hat{e}_L]$ is obtained from the sample covariance

matrix $\hat{\mathbf{R}}_{yy} = \frac{1}{D} \sum_{k=1}^D \mathbf{y}(k) \mathbf{y}^H(k)$. Therefore, the AOA

parameter estimates $(\hat{\theta}_i, \hat{\rho}_{\theta_i})$ of the random and distributed AOAs are given as

$$(\hat{\theta}_i, \hat{\rho}_{\theta_i}) = \arg \min_{\theta_i, \rho_{\theta_i}} p(\theta_i, \rho_{\theta_i}), \quad 1 \leq i \leq L, \tag{13}$$

where the arg min is the argument when the function p gets its minimum. The additional AOA estimates (e.g., azimuth AOA estimate $(\hat{\psi}_i, \hat{\rho}_{\psi_i})$ in Fig. 1) can also be obtained by the same process as the elevation AOA parameter $(\hat{\theta}_i, \hat{\rho}_{\theta_i})$ estimation.

2.4 Completion of VL positioning by data fusion

In order to complete of the short-range VL positioning for smart indoor service, the data fusion process must be advanced successively after the estimation of AOA is finished.

For fusing the obtained AOA estimates, we select the elevation and azimuth center AOA parameters $(\hat{\theta}_i, \hat{\psi}_i)$ among the random distributed AOA parameter estimates $(\hat{\theta}_i, \hat{\rho}_{\theta_i}, \hat{\psi}_i, \hat{\rho}_{\psi_i})$ obtained by the subspace-based AOA estimation technique and determine the receiver position $(\hat{x}_i, \hat{y}_i, \hat{z}_i)$ with the selected estimates $(\hat{\theta}_i, \hat{\psi}_i)$ and the known position (x_i, y_i, z_i) of the i -th VL transmitter by the geometric observation as follows:

$$\hat{\mathbf{X}}_i = \begin{bmatrix} \hat{x}_i \\ \hat{y}_i \\ \hat{z}_i \end{bmatrix} = \begin{bmatrix} r_i \sin \hat{\theta}_i \sin \hat{\psi}_i \\ r_i \sin \hat{\theta}_i \cos \hat{\psi}_i \\ r_i \cos \hat{\theta}_i \end{bmatrix} + \begin{bmatrix} x_i \\ y_i \\ z_i \end{bmatrix} \tag{14}$$

where $r_i^2 = x_i^2 + y_i^2 + z_i^2$, $i = 1, \dots, N$. For a three-dimensional VL positioning environment as in Fig. 1, Eq. (14) can be rewritten as follows in a matrix and vector form:

$$\mathbf{P} \hat{\mathbf{X}}_i = \hat{\mathbf{K}}_i, \tag{15}$$

where $\hat{\mathbf{X}}_i \equiv [\hat{x}_i \ \hat{y}_i \ \hat{z}_i]^T$,

$$\mathbf{P} \equiv \begin{bmatrix} 1 & 0 & 0 \\ 0 & 1 & 0 \\ 0 & 0 & 1 \\ - & - & - \\ \vdots & \vdots & \vdots \\ - & - & - \\ 1 & 0 & 0 \\ 0 & 1 & 0 \\ 0 & 0 & 1 \end{bmatrix}, \tag{16}$$

and

$$\hat{\mathbf{K}}_i \equiv \begin{bmatrix} \hat{\mathbf{X}}_1 \\ \vdots \\ \hat{\mathbf{X}}_N \end{bmatrix} = \begin{bmatrix} r_1 \sin \hat{\theta}_1 \sin \hat{\psi}_1 + x_1 \\ r_1 \sin \hat{\theta}_1 \cos \hat{\psi}_1 + y_1 \\ r_1 \cos \hat{\theta}_1 + z_1 \\ \vdots \\ r_N \sin \hat{\theta}_N \sin \hat{\psi}_N + x_N \\ r_N \sin \hat{\theta}_N \cos \hat{\psi}_N + y_N \\ r_N \cos \hat{\theta}_N + z_N \end{bmatrix}. \tag{17}$$

The three-dimensional position of the receiver in short-range VL positioning for smart indoor services is obtained as

$$\hat{\mathbf{X}} = (\mathbf{P}^T \mathbf{P})^{-1} \hat{\mathbf{K}}. \tag{18}$$

3. Performance Analysis

3.1 Completion of VL positioning by data fusion

We here investigate the characteristics of VL channel in a real positioning environment for smart indoor service, where a VL transmitter radiates VL signal (e.g., LED light

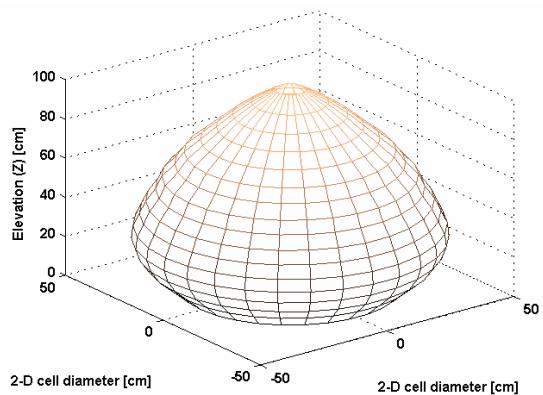


Fig. 4. The surface plot of the three-dimensional VL channel by one VL signal source obtained in a real VL positioning test

of the luminance over 2000 lux) into the air, and a two-dimensional uniform photodiode array acquires the radiated VL signal at different positions.

The three-dimensional positioning VL channel between a VL transmitter and a receiver was measured as follows. A transmitter is fixed at a height of 87cm from the lowest position of the receiver and radiates a VL positioning signal. A uniform photodiode array captures the radiated VL signal at various locations below the transmitter. The receiver moves along the x , y and z directions by 5cm to capture the VL signal. Fig. 4 shows the surface plot of the measured three-dimensional VL channel, inside which an accurate positioning is possible.

From the result in Fig. 4, we can see that the VL channel has the maximum positioning cell size or the maximum receiving area at *quite a few distances* from the bottom (e.g., at a height of 23cm from the bottom in Fig. 4), which means that the selection of the receiver position along the elevation direction is *directly* related to the positioning capability.

Fig. 5 shows the surface plot of the VL channel between three transmitters and a two-dimensional uniform photodiode array receiver in a real environment similar to that depicted in Fig. 1.

We can expect from Fig. 5 that the three sets of AOA parameters of the random and parametric distributed angle form are sometimes available at *arbitrary* positioning cell inside the VL channel generated by three transmitters because of the multipath transfer and short-range travel of VL signal in a short-range VL positioning environment.

3.2 Estimation of AOA parameters

In order to estimate the AOA parameters in the *short-range* VL positioning environment as shown in Fig. 1, we assume that the AOA parameters obtained at the receiver has the random and parametric distributed angle form as shown in Fig. 2 because of the short positioning distance

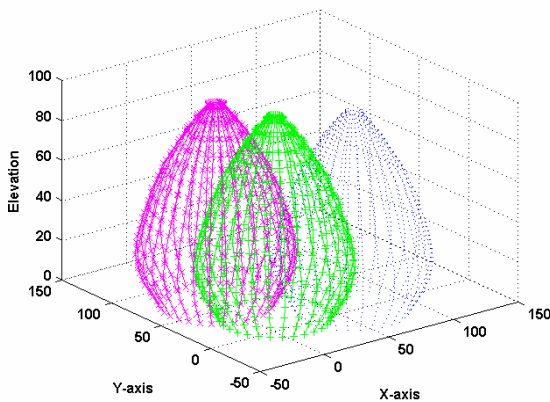


Fig. 5. The surface plot of the three-dimensional VL positioning channels constructed by three VL transmitters in a real VL positioning environment similar to Fig. 1

and the multipath transfer.

The parameter estimation of AOA was executed by the subspace-based estimation technique described in Section 2, and simulations were carried out under the following test conditions: three VL transmitters (i.e., $N = 3$) are at the elevation angle of $\theta_1 = 10^\circ$, $\theta_2 = 50^\circ$, and $\theta_3 = 120^\circ$, respectively, and the VL positioning signals radiated from the three VL transmitters are again acquired at the photodiode array of the VL receiver, where the AOA parameters of the captured signals are of the random and *distributed* angle forms with the Laplace PDF characterized by the center AOA and the spread AOA parameters like Fig. 2(c). The room where the experiment was conducted has a regular tetrahedron shape, the positioning distance is several ten times the photodiode array size of several centimetres, the number of sensors in the photodiode array is $L = 10$, the number of sample data is $D = 500$, and the signal to noise ratio (SNR) is 20 dB.

Through the simulation study for the estimation of AOA parameters in short-range VL positioning for smart indoor service as shown in Fig. 1, the AOA parameters were estimated at the photodiode array of the VL receiver by the proposed subspace-based estimation technique as written in Eq. (13). Fig. 6 shows the inverse plot of the sample null spectrum $p(\theta, \rho_\theta)$. From Fig. 6, we can see that the AOA of the random and distributed angle form with Laplace PDF has three local peaks in the sample null spectrum calculated by the subspace-based estimation technique.

In order to estimate the center AOA parameters of the inverse sample null spectrum in Fig. 6, the three-dimensional sample null spectrum is converted into a two-dimensional one by slicing up the sample spectrum along the spread AOA parameter axis.

Fig. 7 and Fig. 8 show the inverse two-dimensional sample null spectrums under the condition that the spread AOA estimates are given as follows: $\hat{\rho}_\theta = 0.7^\circ, 1.3^\circ, 2.2^\circ$, and $\hat{\rho}_\theta = 0.0^\circ$, respectively

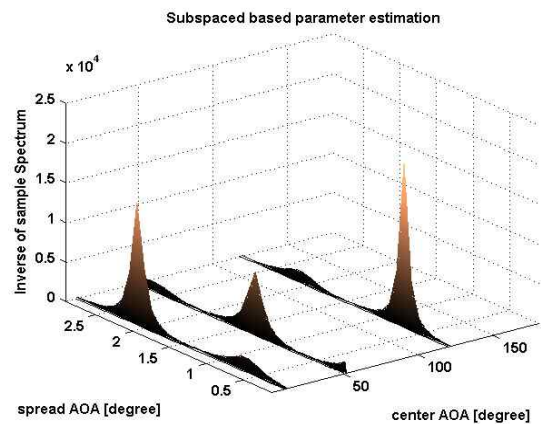


Fig. 6. The inverse plot of the sample null spectrum obtained by the subspace-based AOA estimation technique for short range VL positioning as written in Eq. (13)

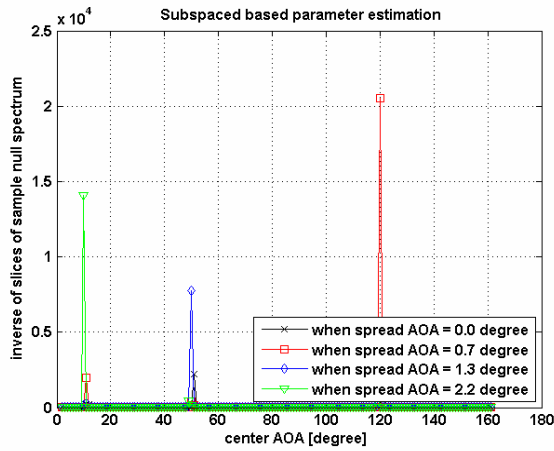


Fig. 7. The inverse plot of the two-dimensional slices of the three-dimensional sample null spectrum of Fig. 6 under the condition that the spread AOA parameter is given

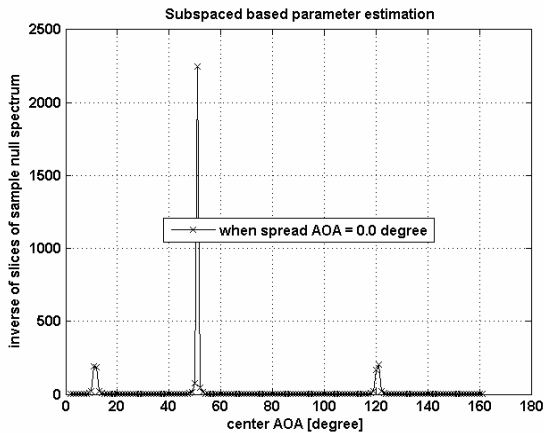


Fig. 8. The inverse plot of the two-dimensional slices of the three-dimensional sample null spectrum of Fig. 6 under the condition that the AOA is assumed the point form like Fig. 2(a)

We can observe from Fig. 7 that the center AOA parameters are obtained from three local peaks of the AOA estimates in Fig. 6 by determining the spread AOA parameter, i.e., $\hat{\theta} = 10^\circ$ under $\hat{\rho}_\theta = 2.2^\circ$, and $\hat{\theta} = 50^\circ$ under $\hat{\rho}_\theta = 1.3^\circ$, and $\hat{\theta} = 120^\circ$ under $\hat{\rho}_\theta = 0.7^\circ$. However, if the AOA of the received VL signal in the short-range VL positioning is assumed to be a point angle form like Fig. 2(a) and so the spread AOA parameter is assumed to be zero, i.e., $\hat{\rho}_\theta = 0.0^\circ$, then the center AOA parameter estimate of one local peak in Fig. 8 comes to have the *wrong* value (i.e., $\hat{\theta} = 52^\circ$) instead of the true AOA parameter, i.e., $\hat{\theta} = 10^\circ$, or $\hat{\theta} = 50^\circ$, or $\hat{\theta} = 120^\circ$, and then the VL positioning *meets* with failure.

3.3 Estimation error

We obtain the estimation error of the random and

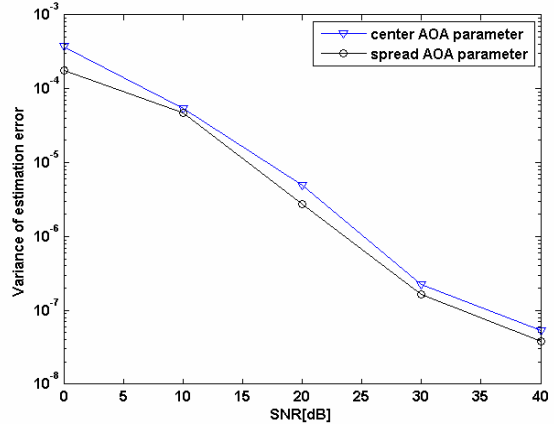


Fig. 9. Variances of the center and spread AOA estimation errors of the subspace-based AOA estimation technique

distributed AOA estimate in order to evaluate the performance of the subspace-based AOA estimation technique.

Since the AOA estimates $(\hat{\theta}_i, \hat{\rho}_{\theta_i})$ in Eq. (13) are the local minima in the three-dimensional sample null spectrum, it is reasonable to assume that $p'(\hat{\theta}_i, \hat{\rho}_{\theta_i}) = 0$. The Taylor series expansion gives that $0 = p'(\hat{\theta}_i, \hat{\rho}_{\theta_i}) \approx p'(\theta_i, \rho_{\theta_i}) + \mathbf{H}(\theta_i, \rho_{\theta_i})\boldsymbol{\varepsilon}_i$, where $\boldsymbol{\varepsilon}_i = [\hat{\theta}_i - \theta_i, \hat{\rho}_{\theta_i} - \rho_{\theta_i}]^T$ is the estimation error vector, $p'(\theta_i, \rho_{\theta_i})$ and $\mathbf{H}(\theta_i, \rho_{\theta_i})$ are the gradient and the Hessian of $p(\theta_i, \rho_{\theta_i})$, respectively. If $\mathbf{H}_i = \lim_{N \rightarrow \infty} \mathbf{H}(\theta_i, \rho_{\theta_i})$ is assumed to be the asymptotic Hessian, then the estimation error becomes $\boldsymbol{\varepsilon}_i = \mathbf{H}_i^{-1} p'(\theta_i, \rho_{\theta_i})$ and the covariance matrix is given as $\mathbf{R}_{\boldsymbol{\varepsilon}\boldsymbol{\varepsilon}} = \mathbf{E}[\boldsymbol{\varepsilon}_i \boldsymbol{\varepsilon}_i^T]$.

The simulation was performed under the following conditions: a uniform photodiode array with ten built-in photodiodes ($L = 10$) and the number of samples was $N = 100$. Three sets of AOA parameters estimated at the receiver were $(\hat{\theta}_1, \hat{\rho}_{\theta_1}) = (10^\circ, 4.3^\circ)$, $(\hat{\theta}_2, \hat{\rho}_{\theta_2}) = (50^\circ, 6.5^\circ)$, and $(\hat{\theta}_3, \hat{\rho}_{\theta_3}) = (120^\circ, 0.6^\circ)$, respectively. The variances of the center AOA and the spread AOA parameter estimates calculated from the relation $\mathbf{R}_{\boldsymbol{\varepsilon}\boldsymbol{\varepsilon}} = \mathbf{E}[\boldsymbol{\varepsilon}_i \boldsymbol{\varepsilon}_i^T]$ were shown in Fig. 9.

From the result in Fig. 9, we can see that both the variance of the estimation error of the center AOA and the spread AOA parameters decrease as the SNR increases, and the variance of the estimation errors of the center AOA parameter are just a little higher than or almost *equal* to those of the spread AOA parameter in the subspace-based estimation technique.

3.4 Data fusion

In order to complete the VL positioning for smart indoor service, the data fusion process must proceed after both the

elevation and azimuth angles of arrival are successively estimated by the subspace-based estimation technique.

We select the elevation and azimuth center AOA parameters $(\hat{\theta}_i, \hat{\psi}_i)$ and determine the receiver position $(\hat{x}_i, \hat{y}_i, \hat{z}_i)$ from Eq. (14) by use of the selected estimates $(\hat{\theta}_i, \hat{\psi}_i)$ and the known position (x_i, y_i, z_i) of the VL transmitters.

4. Conclusion

In short-range VL positioning based on the AOA estimation for smart indoor services, it is expected that the positioning performance mainly depends on the accurate parameter estimation of the AOA of the received signal.

However, the AOA parameters obtained at the receiver are sometimes of a *random* and *distributed* angle form instead of a point angle form in a real VL positioning environment because of multipath transfer and short positioning distance. The AOA parameter estimation for the VL signal of a random and parametric distributed angle form may provide us *incorrect* AOA parameter estimates and result in poor VL positioning performance.

In order to achieve accurate VL positioning in a short-range positioning environment using VL signal having a random and distributed angle form, a short-range VL positioning method and a subspace-based AOA estimation technique were proposed. The performances of the proposed techniques were analysed by measuring the actual VL positioning channel and by simulating the AOA estimation.

The following conclusions were derived from the performance test. The VL channel has the maximum receiving area at a certain distance from the bottom. It is possible to estimate the AOAs of random and parametric distributed angle forms in an arbitrary positioning cell inside the VL channel because of multipath transfer and short-range travel of the received VL positioning signal. The selection of the receiver position in the elevation direction is *directly* related to the positioning capability. If the AOA in short-range VL positioning is assumed to be point angle form, the VL positioning meets with *failure*.

Acknowledgements

This work was supported by the National Research Foundation of Korea (NRF) grant funded by the Korea government (MSIP) (No. 2017R1A2B4002679).

References

- [1] A. Şahin, Y.S. Eroğlu, İ. Güvenç, N. Pala, M. Yüksel, "Hybrid 3-D localization for visible light communication systems," *J. of Light wave Tech.*, vol. 33, pp.

4589 - 4599, 2015.

- [2] S.-H. Yang, E.-M. Jeong, D.-R. Kim, H.-S. Kim, Y.-H. Son, and S.-K. Han, "Indoor three-dimensional location estimation based on LED visible light communication," *Electronics Letters*, vol. 49, pp. 54-56, 2013.
- [3] Q. Yang, X. Zhu, H. Fu, and X. Che, "Survey of security technologies on wireless sensor networks," *Journal of Sensors*, vol. 2015, <http://dx.doi.org/10.1155/2015/842392>, 2015.
- [4] Z. Zhou, M. Kavehrad, and P. Deng, "Indoor positioning algorithm using light-emitting diode visible light communications," *Optical Engineering*, vol. 51, pp.1-6, 2012.
- [5] S. Yang, D. Kim, H. Kim, Y. Son, and S. Han, "Visible light based high accuracy indoor positioning using the extinction ratio distributions of light signals," *Microwave and Optical Technology Letters*, vol. 55, pp.1385-1389, 2013.
- [6] W. Xu, J. Wang, H. Shen, H. Zhang, X. You, "Indoor positioning for Multiphotodiode Device Using Visible-Light Communications," *IEEE Photonics Journal*, vol. 8, pp.1-6, 2016.
- [7] D.H. Johnson and D.E. Dudgeon: *Array signal processing*, Prentice Hall, 1993.
- [8] X. Zhang, K. Cui, M. Yao, H. Zhang, and Z. Xu, "Experimental characterization of indoor visible light communication channels," *IEEE 8th International Symposium on Communication Systems, Networks & Digital Signal Processing*, pp. 1-5, 2012.
- [9] V. Jungnickel, V. Pohl, S. Nönnig, and V. Helmolt, "A physical model for the wireless infrared communication channel," *IEEE J. Sel. Areas in Comm.*, vol. 20, pp. 631-640, 2002.
- [10] T. Komine and M. Nakagawa, "Fundamental analysis for visible-light communication system using LED lights," *IEEE Trans. Consumer Electronics*, vol. 50, pp. 100-107, 2004.
- [11] D. Jung, S. Hann, S. Park, and C. Park, "Optical wireless indoor positioning system using light emitting diode ceiling lights," *Microwave and Optical Technology Letters*, vol. 54, pp. 1622-1626, 2012.
- [12] Y.U. Lee and S.M. Lee, "Random distributed angle-of-arrival parameter estimation technique for visible light positioning," *IEEE 38th International Conference of Telecommunications and Signal Processing (TSP)*, vol. 58, pp. 467-471, 2015.



Yong Up Lee He is with the Hallym University Dept. of Electronic Engineering as a professor. He has over 70 published papers, books, patents. His research interests are in the areas of wireless and optical communications. He has received the B.S. degree in

electronics engineering from Seoul National University, Seoul, Korea, in 1985, and the M.S. and Ph.D. degrees in electrical engineering from KAIST, Daejeon, Korea, in 1987 and 1996, respectively. He was a researcher at Samsung Electronics, Institute of Information and Telecommunication, Korea, from 1987 to 1998. He visited with the Department of Electrical Engineering, University of New South Wales, Sydney, NSW, Australia, from December 2013 to December 2014, and CCITR, the Department of Electrical Engineering, Pennsylvania State University, University Park PA, USA, from August 2011 to May 2012.



Seop Hyeong Park He received B.S., M.A., and Ph.D. degrees from Seoul National University, Korea, in 1984, 1986, and 1990, respectively, all in electrical engineering. From 1990 to 1992, he was with the HDTV Development Center, Korean Academy of Industrial Technology, where he

worked on the design and implementation of an HDTV decoder. From 1992 to 1998, he was with Korea Telecom, where he worked on digital video compression, multimedia service management software, video on demand and video conferencing service over ATM networks. In 1993, he was a visiting researcher at the NTT Human Interface Laboratory, Yokosuka, Japan, where he worked on post-processing of compressed HDTV video signals. He joined Hallym University, Gangwon-do, Korea, in 1998, where he is currently a Professor in the Department of Electronic Engineering. In 2004, he was a visiting scholar at the University of California, Santa Barbara. From 2006 to 2009, he was the dean of College of Information and Electronics, Hallym University. In 2011, He was a visiting professor at Mongolia International University. His research interests are signal processing including speech, video and ultrasound signals, multimedia communication, and machine learning.